Spin crossover in liquid (Mg,Fe)O at extreme conditions

E. Holmström[1,2,*] and L. Stixrude[1]

[1]*Department of Earth Sciences, University College London, Gower Street, London WC1E 6BT, United Kingdom*

[2]*Department of Applied Physics, COMP Centre of Excellence, Aalto University, P.O. Box 11100, 00076 Aalto, Espoo, Finland*

(Received 21 December 2015; revised manuscript received 4 May 2016; published 20 May 2016)

We use first-principles free-energy calculations to predict a pressure-induced spin crossover in the liquid planetary material (Mg,Fe)O, whereby the magnetic moments of Fe ions vanish gradually over a range of hundreds of GPa. Because electronic entropy strongly favors the nonmagnetic low-spin state of Fe, the crossover has a negative effective Clapeyron slope, in stark contrast to the crystalline counterpart of this transition-metal oxide. Diffusivity of liquid (Mg,Fe)O is similar to that of MgO, displaying a weak dependence on element and spin state. Fe-O and Mg-O coordination increases from approximately 4 to 7 as pressure goes from 0 to 200 GPa. We find partitioning of Fe to induce a density inversion between the crystal and melt, implying separation of a basal magma ocean from a surficial one in the early Earth. The spin crossover induces an anomaly into the density contrast, and the oppositely signed Clapeyron slopes for the crossover in the liquid and crystalline phases imply that the solid-liquid transition induces a spin transition in (Mg,Fe)O.

DOI: 10.1103/PhysRevB.93.195142

I. INTRODUCTION

Planets with an Earth-like, rock-dominated composition tend to be partially or entirely molten at the early stages of their evolution [1,2]. This is due to the large amounts of energy deposited into the early planet during the accretion process through which the body is formed. In particular, giant impacts involving impactors of $>10\%$ of the planet's mass are thought to be a generic part of the accretion process, an example being the Moon-forming impact on the early Earth [3]. How the initial magma ocean crystallizes determines the starting conditions for the growth and evolution of the lithosphere, hydrosphere, and atmosphere of the planet [1,4,5]. In order to quantitatively understand the crystallization of the magma ocean, it is necessary to know the properties of molten planetary materials at the high pressures and temperatures relevant to the process. Experimental work utilizing shock-wave experiments [6], and the laser-heated diamond anvil cell [7] has produced valuable results, but many properties of these liquids remain weakly constrained. Quantum-mechanical, finite-temperature density-functional theory (DFT) molecular dynamics (MD) [8,9] has proved to be a powerful and accurate theoretical method for predicting the properties of liquid silicates [10–13], oxides [14,15], and metals [16] at extreme conditions. In this approach, no assumptions are made on the shape of the electronic charge density, and the effects of temperature are included in both the electronic and ionic degrees of freedom.

Spin crossover is a phenomenon whereby the spin states of transition-metal ions or complexes are altered due to applied pressure, temperature, or photon irradiation [17]. The phenomenon has been observed in solids, liquids, liquid crystals, and complexes in solution [18] and is believed to enable a wide array of technological applications from switching-devices to sensors [17]. Spin crossover has been shown to accompany a solid-to-liquid phase transition in some systems [19], and a different threshold temperature for spin crossover in the solid phase compared to a liquid crystal phase of the same complex has been reported [20]. While the crossover in crystalline planetary materials has received much attention in recent years [21–25], the question of a spin crossover in the liquid phase of these materials is little explored to date [7,26].

We have recently developed a new *ab initio* method for studying spin crossover phenomena. This method was tested with great success for crystalline (Mg,Fe)O against the abundant experimental data available for this phase [25]. The method is general and applicable to both solids and liquids. In the present paper, we explore the extent to which liquid phase behavior for (Mg,Fe)O differs from that of the crystalline phase.

In this paper, we use finite-temperature DFT MD coupled with free-energy calculations to predict a spin crossover in liquid (Mg,Fe)O, the molten phase of the prevalent planetary material ferropericlase. The low-pressure, magnetic high-spin state of Fe in this transition-metal oxide is formed by four unpaired $3d$ electrons ($S = 2$) and the nonmagnetic low-spin state by a fully paired valence shell ($S = 0$). As pressure increases, we find a growing fraction of the Fe ions to assume the low-spin state, with a mixed-spin phase of coexisting high-spin and low-spin Fe dominating the phase diagram up to 10 000 K and 200 GPa. Whereas in crystalline (Mg,Fe)O the effective Clapeyron slope of the spin crossover is positive, we find the slope to be *negative* in the liquid phase. This remarkable finding implies that melting can induce a spin crossover in (Mg,Fe)O, and the oppositely signed Clapeyron slopes on the two sides of the solid-liquid transition of (Mg,Fe)O furthermore cause an anomaly in the density contrast between coexisting crystal and melt. We predict a density inversion of crystal and melt upon partitioning of Fe between the two phases, which implies separation of a basal magma ocean from a surficial one in the early Earth. Finally, we find liquid (Mg,Fe)O to exhibit electrical conductivity high enough to power a geodynamo within the early Earth and persistently within extra-solar super-Earths.

*eero.holmstrom@aalto.fi

 ©2016 American Physical Society

II. METHODOLOGY

We perform our DFT MD computations using the VASP simulation package [27]. Our model system is a cubic supercell of 128 ions of $(Mg_{1-x},Fe_x)O$ with an Fe concentration of $x = 25\%$, with periodic boundary conditions applied in all dimensions. For keeping the simulations precise yet efficient, we sample the Brillouin zone at the Baldereschi point [8,28] for a lattice of simple cubic symmetry and use a plane-wave cutoff energy of 500 eV. Further efficiency is obtained by using the projector-augmented wave method to represent the ionic core potentials. We use the PBEsol functional [29] to approximate the quantum-mechanical exchange and correlation many-body effects of the system of electrons. In order to account for the strong correlation between the Fe $3d$ electrons, we augment PBEsol through the $+U$ methodology [30], choosing $U - J = 2.5$ eV. This approach to computing the exchange and correlation energy was recently shown to give results on the equation of state and spin crossover in crystalline (Mg,Fe)O in excellent agreement with experiment [25]. We run our spin-polarized PBEsol + U MD simulations in the NVT ensemble using the Nosé-Hoover thermostat. For good conservation of energy, we choose a time step of 0.5 fs for integrating the ionic equations of motion. To prepare initial structures at the supercell volumes V applied in the simulations, we melt an initially perfect crystal structure of (Mg,Fe)O in the B2 phase at 10 000 K, followed by 3 ps of MD at each value of V, which produces a fully equilibrated liquid at each compression. The chosen range of compressions results in pressures of approximately 0 to 300 GPa. We take the last frame of each of these initial simulations as input for the initial structure for each of the isotherms in our production runs ($T = 6000$, 8000, and 10 000 K). Each simulation is then first run for a duration of 2 ps, during which thermal equilibrium is reached. This is followed by another 3 ps of simulation, over which all physical time averages are computed. These temperatures and pressures encompass typical conditions in newly accreted terrestial planets as well as prevailing conditions inside super-Earths [2].

For finding the stable mean magnetic moment at a given pressure and temperature, i.e., to produce a phase diagram of the spin crossover in liquid (Mg,Fe)O, we harness the free-energy minimization approach introduced in our recent work on crystalline (Mg,Fe)O [25]. In this method, for each isotherm, we consider four different spin phases: one with all Fe ions in the high-spin state, one with all Fe in the low-spin state, and two mixed-spin phases, each with a different mean magnetic moment on the Fe ions intermediate between vanishing and that in the high-spin phase. The ion-specific magnetic moments are not as well-defined in the liquid as they are in the crystalline phase [31], but to quantify the spin crossover, we choose to use the same quantity as in the case of the crystal, that is, $f = \langle|\mu_{Fe}|\rangle/\langle|\mu_{Fe}^{HS}|\rangle$, where μ_{Fe} and μ_{Fe}^{HS} denote the Fe magnetic moment and the same in the high-spin phase, respectively, and $\langle\rangle$ denotes an average over Fe ions and time. The computational effort of the method is concentrated on finding $\Delta G(P,T,f) = G(P,T,f) - G(P,T,0)$ and minimizing this with respect to f, here $G(P,T,f) = H - TS$ being the Gibbs free energy of the liquid. The enthalpy H of a given phase is obtained directly from the MD simulations. To find the entropic contribution $T\Delta S$, we break the entropy down to $S = S_{\rm conf} + S_{el} + S_{\rm mag}$. Here $S_{\rm conf}$ is the configurational entropy due to nuclear excursions of the ions in the liquid as well as the entropy from site-switching of high-spin and low-spin moments among the Fe ions. S_{el} is the electronic entropy due to finite electronic temperature [27,32] (this being set equal to the ionic temperature), and $S_{\rm mag}$ is the entropy due to the paramagnetic state of the moments in the liquid, with full disorder expected at the chosen simulation conditions [33]. To find $S_{\rm conf}$, we use adiabatic switching, a form of thermodynamic integration [34,35]. We obtain S_{el} directly from the simulation, and $S_{\rm mag}$ we compute from the expression [36] $S_{\rm mag} = k_B \sum_i \ln(|\mu_i| + 1)$, where μ_i is the total magnetic moment of Fe ion i, and k_B is the Boltzmann constant. Finally, to find the equilibrium f at any P and T, we interpolate $\Delta G = \Delta G(f)$ using a free second-order polynomial [31].

III. RESULTS AND DISCUSSION

A. Phase diagram for the spin crossover

Our first-principles phase diagram for the spin crossover in liquid (Mg,Fe)O is presented in Fig. 1. At low pressures, the Fe ions are all in the high-spin state, as expected from Hund's first rule. However, compression of the liquid makes the high-spin configuration less and less favorable through broadening of the electronic bands [37] as well as the $P\Delta V$ contribution to the free energy favoring the smaller low-spin Fe ion [38,39]. With increasing pressure, the liquid is driven into a mixed-spin phase of coexisting high-spin and low-spin ions, with the mean moment approaching approximately one half that of the high-spin value towards $P = 200$ GPa. The crossover thus appears extremely broad, as was found recently for another Fe-bearing liquid planetary material Fe_2SiO_4 [26] from direct DFT MD without considering the full Gibbs free energy. The breadth of the spin crossover region of at least hundreds of GPa in the liquid contrasts with that in the crystalline phase where the crossover is much sharper: High-spin and low-spin Fe coexist over a range of pressure of ∼50 to 150 GPa. We attribute this difference to a much higher configurational entropy of the mixed-spin phase in the liquid, originating in the larger variety of coordination environments available to Fe in the liquid state. The free energy of mixing ($\Delta G_{\rm mix}$) of high-spin and low-spin ions is approximately −50 meV/atom within the crossover at all temperatures, with the enthalpy and each contribution to the

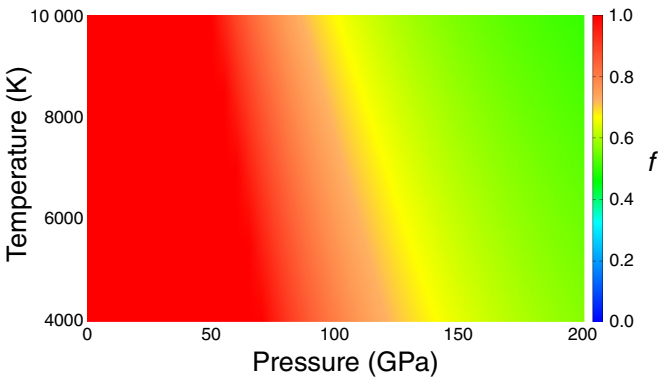

FIG. 1. Phase diagram of the spin crossover in liquid (Mg,Fe)O.

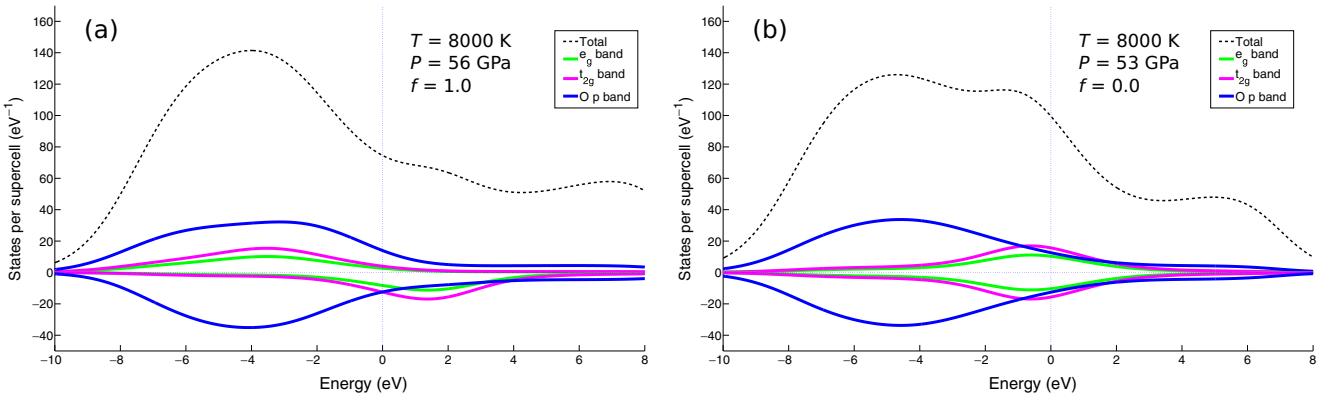

FIG. 2. Electronic density of states of liquid (Mg,Fe)O at 8000 K and intermediate pressure, for (a) $f = 1.0$ and (b) $f = 0.0$. The spin-up channel of the DOS is plotted as positive values, the spin-down channel as negative values, and the total DOS as positive values. The Fermi level is at $E = 0$ eV.

entropy separately favoring mixing. We find full disordering of the moments, i.e., no short-range spin-spin ordering. However, it is reasonable to assume that the mixture of large and small Fe ions (high-spin and low-spin, respectively) gives rise to the observed favorable enthalpy of mixing, as was found for the crystalline phase [25].

A prominent feature of the phase diagram is the shrinking of the high-spin stability regime with increasing temperature. The slope dP/dT of the $f = 0.5$ isopleth can thus be thought to define an effective Clapeyron slope for the spin crossover which is negative (-0.014 GPa/K). This finding represents a stark contrast to the crystalline phase of (Mg,Fe)O, where the slope of the $f = 0.5$ isopleth is characterized by a positive value (0.018 GPa/K) [25]. The present feature in the liquid phase diagram is due to the electronic entropy S_{el} favoring low-spin Fe, and S_{el} itself and hence TS_{el} undergoing a strong increase with temperature. This is because in the low-spin state, Fe contributes more electronic states to the system near the Fermi level than in the high-spin state, and an increase in temperature serves to further increase the density of states in this energy region (Fig. 2). The increase in TS_{el} with temperature dominates over the simultaneous increase in magnetic entropy TS_{mag}, the latter favoring high-spin Fe, the net result being the observed negative Clapeyron slope.

B. Diffusivity

We determine the total self-diffusion coefficient D of (Mg,Fe)O from the mean-squared displacements of the ions using Einstein's law [40]. The results and their fit to the Arrhenius relation [41]

$$D(P,T) = D_0 e^{-(E_a + PV_a)/k_B T} \quad (1)$$

with parameters $D_0 = 459 \times 10^{-9}$ m^2/s, $E_a = 1.16$ eV, $V_a = 1.21$ Å^3 are presented in Fig. 3. The diffusivity of (Mg,Fe)O appears thus overall fairly similar to that of MgO [15], the small but systematic difference being possibly attributable to the difference in exchange-correlation functional (PBEsol + U vs LDA) and the different chemical composition. The diffusivities of high-spin Fe, low-spin Fe, Mg, and O reveal a weak dependence of D on element and spin state [31], the weak dependence on spin state being at odds with earlier results on Fe diffusivity in crystalline (Mg,Fe)O, where the diffusivity was found to vary by a factor of three between high-spin and low-spin Fe [42]. We attribute the different behavior in the liquid to the much larger variety of coordination states and diffusive transition states available as compared with the crystal.

C. Mechanical properties

The equation of state (EOS) is presented in Fig. 4 for all studied isotherms. The large width of the crossover entails no inflections directly attributable to the spin crossover, contrary to the case of the crystalline equation of state [25]. At high pressures, we find good agreement with experimental shock-wave data on $Mg_{0.6}Fe_{0.4}O$ [43]. While it is unclear whether the experimental sample is molten at these conditions, a volume discontinuity found in the Hugoniot of $Mg_{0.6}Fe_{0.4}O$ at 145 GPa is consistent with a solid-liquid transition of the crystal [44]. The temperature in these experiments increases on compression and is not measured. The porous nature of the starting material means that the temperature likely exceeds melting at the highest pressure conditions. The experimental

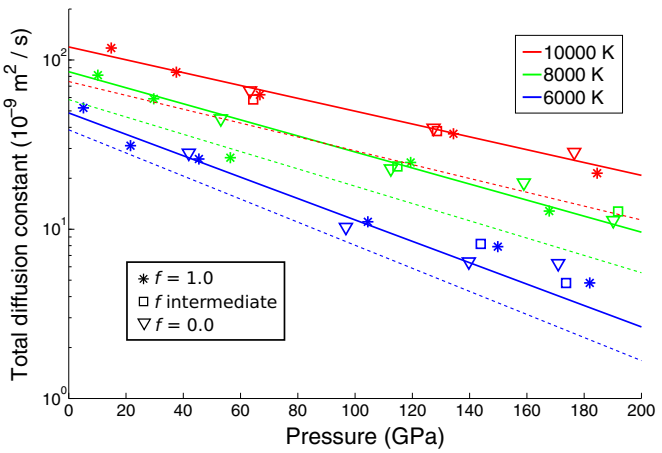

FIG. 3. Total diffusivity with Arrhenius fits (solid lines, see text) as well as Arrhenius fits for MgO from local-density approximation DFT MD (dashed lines) [15].

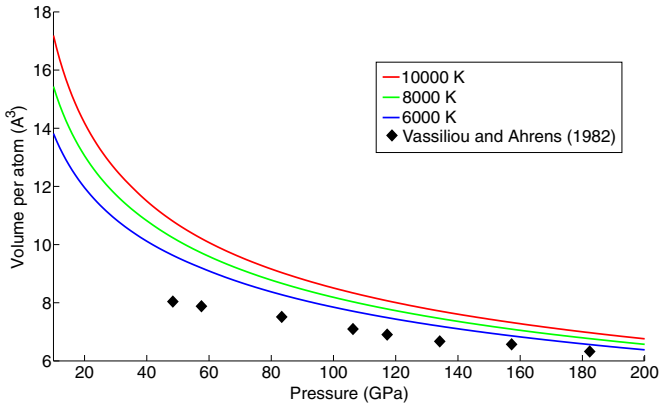

FIG. 4. Equation of state of liquid (Mg,Fe)O over all the simulated isotherms, as given by the spin crossover, along with experimental shock-wave data from Ref. [43] (see text).

volume at 183 GPa is slightly less than what we find at 6000 K, consistent with the experimental temperature being somewhat lower than 6000 K.

We calculate the Fe-O and Mg-O mean coordination numbers $\langle Z_{\mathrm{FeO}}\rangle$ and $\langle Z_{\mathrm{MgO}}\rangle$ from

$$\langle Z_{XO}\rangle = \rho_0 \int_0^{r_{\min}} g_{XO}(r) 4\pi r^2 dr, \qquad (2)$$

where $g_{XO}(r)$ is the corresponding partial radial distribution function and ρ_0 the total number density of O. The upper limit of the integral is set to the radius corresponding to the first minimum in $g(r)$ after the first peak, in order for the ensuing $\langle Z\rangle$ to approximate the first-neighbor coordination shell. From the results, plotted in Fig. 5, we find increasing coordination from ~4 to 6 for Fe-O and 4 to 7 for Mg-O over the volume range considered here. It has been shown that number density rather than pressure or temperature is crucial to the structure of silicate liquids [48], and therefore we compare our coordination numbers to experiments at the same number density. We find $\langle Z_{\mathrm{FeO}}\rangle \approx 4.5$ at 13.1 Å^3/atom, which is close to the experimental value of 5.2 at the same mean atomic volume in FeO-SiO_2 liquid at the limit of low-SiO_2 content [45,46]. We find a higher result for $\langle Z_{\mathrm{FeO}}\rangle$ by as much as 1.0 when Fe is in the high-spin state as compared to the low-spin state, which reflects the larger spatial extent of the 3*d*-like orbitals in the former electronic configuration and hence a larger ionic radius. The Mg-O coordination is very close to previous *ab initio* results on pure MgO [15] and appears independent of the spin state of Fe in the liquid. We find $\langle Z_{\mathrm{MgO}}\rangle \approx 5.2$ at 11.4 Å^3/atom, very close to the experimental value of 4.95 at the same atomic volume [47].

D. Spin crossover and the solid-liquid transition

By combining our present results on the spin crossover with previous data on crystalline (Mg,Fe)O [25], and by treating crystalline and liquid (Mg,Fe)O each as an ideal solution of MgO and FeO [31,49], we construct a composite phase diagram for the spin crossover over both the crystalline and liquid PT stability range (Fig. 6). The oppositely-signed dP/dT for the crystal and melt are clearly visible. A remarkable prediction of this composite phase diagram is the steep decrease in f upon melting at pressures of 100 to 130 GPa, showing that spin crossover can be induced in (Mg,Fe)O by the solid-liquid phase transition.

A prevailing question related to the crystallization of a terrestial magma ocean is the density contrast between the coexisting crystalline and liquid phases [4]. A melt denser than the crystal will sink, facilitating the birth of a basal magma ocean [5], with important consequences for the geochemistry of the planet. From our ideal solution analysis, we find $x \approx 0.05$ in crystalline (Mg,Fe)O along the liquidus, in excellent agreement with recent experimental data [50]. By assuming the mean atomic volume to be unchanged upon altering the Fe fraction, we estimate the density of (Mg,Fe)O along the liquidus. The ensuing densities of the coexisting crystal and melt and the density contrast are presented in Figs. 7(a) and 7(b), respectively, for both the isochemical ($x = 0.25$ in each phase) and Fe-partitioned case. It can be clearly seen that the compositional difference between the two phases upon partitioning of Fe is what controls the density contrast, as found earlier for (Mg,Fe)SiO_3 [52]. The melt is predicted to be denser than the crystal throughout the entire stability range of crystalline (Mg,Fe)O, which implies crystal flotation in the early magma ocean and separation of a basal magma ocean from a surficial one [5,52]. The spin crossover has a small but noticeable effect on the density contrast. In comparison

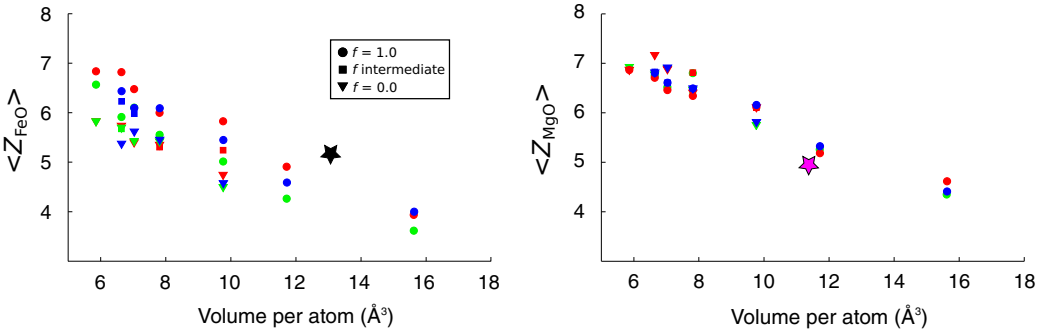

FIG. 5. Mean Fe-O and Mg-O coordination numbers in liquid (Mg,Fe)O over all simulated volumes. Colors are for temperature, with red indicating $T = 10\,000$ K, green $T = 8000$ K, and blue $T = 6000$ K. The black star indicates the experimental result at $T = 1573$ K for FeO-SiO_2 at the compositional limit of low SiO_2 content [45,46], and the magenta star indicates the experimental result for quenched Mg_2SiO_4 glass [47].

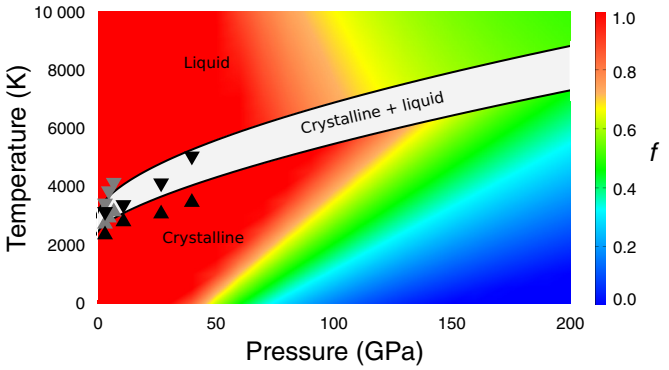

FIG. 6. Composite phase diagram of the spin crossover in crystalline and liquid (Mg,Fe)O. Upward and downward pointing triangles denote experimental solidus and liquidus temperatures, respectively, with black symbols from measurements of Du and Lee [50] and gray symbols from measurements of Zhang and Fei [51].

to the hypothetical case of no spin crossover ($f = 1$ for all P,T), the lower onset pressure of the spin crossover in the liquid causes an increase in the density contrast at around 70 to 120 GPa, an effect which is mirrored in the crystalline phase at higher pressures upon the onset of the crossover in the crystal.

E. Electrical conductivity

Finally, we compute the total electronic conductivity (σ) of liquid (Mg,Fe)O by employing the Nernst-Einstein relation [53] for the ionic component ($\sigma_{\rm ion}$) and the Kubo-Greenwood method [54,55] for the electronic component (σ_{el}). At 8000 K and 56 GPa, we find $\sigma_{\rm ion} \approx 2.5 \times 10^3$ S/m and $\sigma_{el} \approx 1.0 \times 10^5$ S/m, the electronic density of states displaying no band gap [31]. Our result $\sigma \approx 10^5$ S/m is similar to experimentally based estimates of the conductivity of other liquid planetary materials, such as MgO ($>10^4$ S/m) [6], SiO_2 (10^4 to 10^5 S/m) [56], and $MgSiO_3$ ($>10^5$ S/m) [57], noting though that some of these experiments were performed at higher temperatures and pressures [6,57]. The predicted (nearly) metallic conductivity of liquid (Mg,Fe)O raises the possibility that as a component of an early basal magma ocean, the material may have functioned to give rise to a magnetic field on Earth long before the onset of the present core dynamo mechanism [58]. The role of (Mg,Fe)O and other liquid oxides as a source of dynamo action in Earth is likely historical, and may be preserved in the geological record, providing a test of the existence of a magma ocean. Magma oceans may persist inside super-Earths for much longer times [2], granting a plausible and generic mechanism for magnetic-field generation in these large, extra-solar bodies.

IV. CONCLUSIONS

Using DFT MD in conjunction with free-energy calculations, we predict a pressure-induced spin crossover in liquid (Mg,Fe)O. The crossover is found to be hundreds of GPa in width, much broader than in the crystalline phase of this transition-metal oxide. In addition, the crossover exhibits a negative Clapeyron slope, again in contrast to the crystalline phase. The different character of the spin crossover in the two phases of (Mg,Fe)O leads to a spin transition induced by melting as well as an anomaly in the density contrast between coexisting crystal and melt. Finally, we predict near-metallic electrical conductivity for the material, the electronic component dominating over the ionic one, implying a role for (Mg,Fe)O in magnetic-field generation in the early Earth as well as super-Earths.

In terms of better understanding the early Earth, it will be important to evaluate how the addition of other components affects the spin crossover in liquid (Mg,Fe)O. The addition of SiO_2 is expected to raise spin transition pressures, as is the case for crystalline (Mg,Fe)O vs (Mg,Fe)SiO_3 [59]. Consistent with this expectation, higher mean Fe moments were found previously in Fe_2SiO_4 melt compared to the present results in (Mg,Fe)O (3.2 μ_B vs 2.1 μ_B at 6000 K and 136 GPa, respectively).

The first-principles free-energy method that we employ in this and earlier work [25] to predict the stable high-spin fraction $f(P,T)$ has now been successfully demonstrated for both crystalline and liquid systems. The approach seems general and robust, being free of the constraints of earlier methods relying on lattice dynamics and negligible Fe-Fe interactions [60,61]. We therefore anticipate our method to

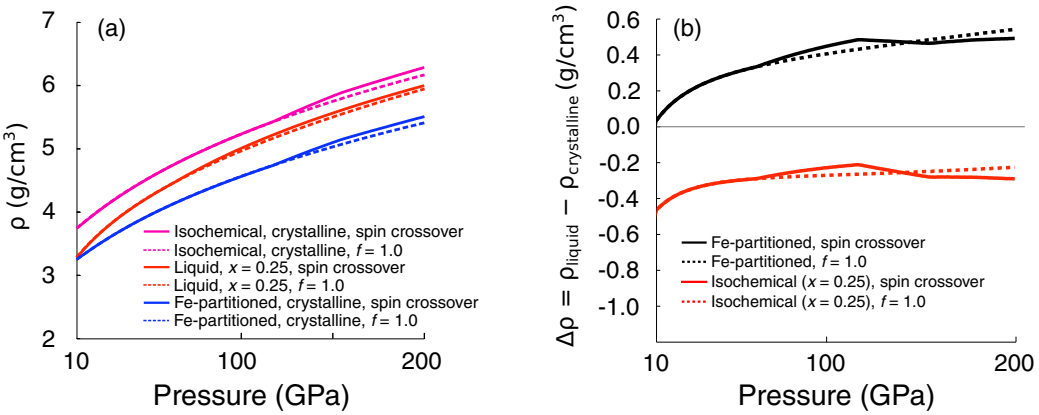

FIG. 7. (a) Densities of the crystal and melt along the liquidus. (b) Density contrast between the (Mg,Fe)O crystal and melt along the liquidus.

be useful for various Fe-rich systems (including pure liquid Fe) in mineral physics and more generally condensed-matter physics at extreme conditions.

ACKNOWLEDGMENTS

Research supported by the European Research Council under Advanced Grant No. 291432 "MoltenEarth" (FP7/2007-2013). Calculations were performed on the Iridis computing cluster partly owned by University College London, and HECToR and ARCHER of the UK national high-performance computing service. We acknowledge financial support by the Academy of Finland through the Centres of Excellence Program (Project No. 251748). The authors acknowledge helpful comments from R. E. Cohen, K. K. M. Lee, and R. Jeanloz.

[1] C. B. Agee and D. Walker, Earth Plan. Sci. Lett. **90**, 144 (1988).
[2] L. Stixrude, Phil. Trans. R. Soc. A **372**, 20130076 (2014).
[3] R. M. Canup and E. Asphaug, Nature Lett. **412**, 708 (2001).
[4] C. B. Agee, Phys. Earth Plan. Int. **107**, 63 (1998).
[5] S. Labrosse, J. W. Hernlund, and N. Coltice, Nature Lett. **450**, 866 (2007).
[6] R. S. McWilliams, D. K. Spaulding, J. H. Eggert, P. M. Celliers, D. G. Hicks, R. F. Smith, G. W. Collins, and R. Jeanloz, Science **338**, 1330 (2012).
[7] R. Nomura, H. Ozawa, S. Tateno, K. Hirose, J. Hernlund, S. Muto, H. Ishii, and N. Hiraoka, Nature Lett. **473**, 199 (2011).
[8] R. M. Martin, *Electronic Structure: Basic Theory and Practical Methods* (Cambridge University Press, Cambridge, England, 2008).
[9] D. Marx and J. Hutter, *Ab Initio Molecular Dynamics: Basic Theory and Advanced Methods* (Cambridge University Press, Cambridge, England, 2012).
[10] L. Stixrude and B. Karki, Science **310**, 297 (2005).
[11] B. B. Karki and L. P. Stixrude, Science **328**, 740 (2010).
[12] N. de Koker, B. B. Karki, and L. Stixrude, Earth and Plan. Sci. Lett. **361**, 58 (2013).
[13] B. Boates and S. A. Bonev, Phys. Rev. Lett. **110**, 135504 (2013).
[14] D. Alfe, Phys. Rev. Lett. **94**, 235701 (2005).
[15] B. B. Karki, D. Bhattarai, and L. Stixrude, Phys. Rev. B **73**, 174208 (2006).
[16] D. Alfe, G. D. Price, and M. J. Gillan, Phys. Rev. B **65**, 165118 (2002).
[17] A. Bousseksou, G. Molnár, L. Salmon, and W. Nicolazzi, Chem. Soc. Rev. **40**, 3313 (2011).
[18] Y. Bodenthin, G. Schwarz, Z. Tomkowicz, T. Geue, W. Haase, U. Pietsch, and D. G. Kurth, J. Am. Chem. Soc. **131**, 2934 (2009).
[19] D. Kiriya, H.-C. Chang, and S. Kitawaga, J. Am. Chem. Soc. **130**, 5515 (2008).
[20] K. Kuroiwa, H. Kikuchi, and N. Kimizuka, Chem. Commun. **46**, 1229 (2010).
[21] J. Badro, G. Fiquet, F. Guyot, J.-P. Rueff, V. V. Struzhkin, G. Vanko, and G. Monaco, Science **300**, 789 (2003).
[22] J. Badro, J.-P. Rueff, G. Vanko, G. Monaco, G. Fiquet, and F. Guyot, Science **305**, 383 (2004).
[23] J.-F. Lin, G. Vanko, S. D. Jacobsen, V. Iota, V. V. Struzhkin, V. B. Prakapenka, A. Kuznetsov, and C.-S. Yoo, Science **317**, 1740 (2007).
[24] Z. Mao, J.-F. Lin, J. Liu, and V. B. Prakapenka, Geophys. Res. Lett. **38**, L23308 (2011).
[25] E. Holmström and L. Stixrude, Phys. Rev. Lett. **114**, 117202 (2015).
[26] D. M. Ramo and L. Stixrude, Geophys. Res. Lett. **41**, 4512 (2014).
[27] G. Kresse and J. Hafner, Phys. Rev. B **47**, 558(R) (1993); **49** 14251 (1994); G. Kresse and J. Furthmüller, Comput. Mat. Sci. **6**, 15 (1996); Phys. Rev. B, **54**, 11169 (1996).
[28] A. Baldereschi, Phys. Rev. B **7**, 5212 (1973).
[29] J. P. Perdew, A. Ruzsinsky, G. I. Csonka, O. A. Vydrov, G. E. Scuseria, L. A. Constantin, X. Zhou, and K. Burke, Phys. Rev. Lett. **100**, 136406 (2008).
[30] S. L. Dudarev, G. A. Botton, S. Y. Savrasov, C. J. Humphreys, and A. P. Sutton, Phys. Rev. B **57**, 1505 (1998).
[31] See Supplemental Material at http://link.aps.org/supplemental/10.1103/PhysRevB.93.195142 for details of the free energy computations, magnetic moment distributions, diffusivity results, and the ideal solution analysis for constructing the joint crystalline-liquid phase diagram of (Mg,Fe)O.
[32] N. D. Mermin, Phys. Rev. **137**, A1441 (1965).
[33] S. Speziale, A. Milner, V. E. Lee, S. M. Clark, M. P. Pasternak, and R. Jeanloz, PNAS **102**, 17918 (2005).
[34] L. Vocadlo and D. Alfe, Phys. Rev. B **65**, 214105 (2002).
[35] M. J. Gillan, D. Alfe, J. Brodholt, L. Vocadlo, and G. D. Price, Rep. Prog. Phys. **69**, 2365 (2006).
[36] G. Grimvall, Phys. Rev. B **39**, 12300 (1989).
[37] R. E. Cohen, I. I. Mazin, and D. G. Isaak, Science **275**, 654 (1997).
[38] K. Persson, A. Bengtson, G. Ceder, and D. Morgan, Geophys. Res. Lett. **33**, L16306 (2006).
[39] J. C. Crowhurst, J. M. Brown, A. F. Goncharov, and S. D. Jacobsen, Science **319**, 451 (2008).
[40] N. W. Ashcroft and N. D. Mermin, *Solid State Physics* (Saunders College, Philadelphia, 1976).
[41] P. Atkins and J. de Paula, *Atkins' Physical Chemistry* (W. H. Freeman and Company, New York, 2006).
[42] M. Ammann, J. P. Brodholt, and D. P. Dobson, Earth and Plan. Sci. Lett. **302**, 393 (2011).
[43] M. S. Vassiliou and T. J. Ahrens, Geophys. Res. Lett. **9**, 127 (1982).
[44] L. Zhang, Z. Gong, and Y. Fei, J. Phys. Chem. Sol. **69**, 2344 (2008).
[45] Y. Waseda and J. M. Toguri, Metall. Trans. B **9B**, 595 (1978).
[46] Y. Shiraishi, K. Ikeda, A. Tamura, and T. Saito, Trans. JIM **19**, 264 (1978).
[47] S. Kohara, Science **303**, 1649 (2004).
[48] N. Sun, L. Stixrude, N. de Koker, and B. B. Karki, Geoch. Cosm. Acta **75**, 3792 (2011).
[49] L. Stixrude, J. Geophys. Res. **102**, 14835 (1997).
[50] Z. Du and K. K. M. Lee, Geophys. Res. Lett. **41**, 8061 (2014).
[51] L. Zhang and Y. Fei, Geophys. Res. Lett. **35**, L13302 (2008).

[52] L. Stixrude, N. de Koker, N. Sun, M. Mookherjee, and B. B. Karki, Earth and Plan. Sci. Lett. **278**, 226 (2009).
[53] M. Mookherjee, L. Stixrude, and B. Karki, Nature Lett. **452**, 983 (2008).
[54] M. Pozzo, M. P. Desjarlais, and D. Alfe, Phys. Rev. B **84**, 054203 (2011).
[55] M. P. Desjarlais, J. D. Kress, and L. A. Collins, Phys. Rev. E. **66**, 025401(R) (2002).
[56] D. G. Hicks, T. R. Boehly, J. H. Eggert, J. E. Miller, P. M. Celliers, and G. W. Collins, Phys. Rev. Lett. **97**, 025502 (2006).
[57] D. K. Spaulding, R. S. McWilliams, R. Jeanloz, J. H. Eggert, P. M. Celliers, D. G. Hicks, G. W. Collins, and R. F. Smith, Phys. Rev. Lett. **108**, 065701 (2012).
[58] L. B. Ziegler and D. R. Stegman, Geochem. Geophys. Geosys. **14**, 1 (2013).
[59] J.-F. Lin, S. Speziale, Z. Mao, and H. Marquardt, Rev. Geophys. **51**, 244 (2013).
[60] T. Tsuchiya, R. M. Wentzcovitch, C. R. S. da Silva, and S. de Gironcoli, Phys. Rev. Lett. **96**, 198501 (2006).
[61] R. M. Wentzcovitch, J. F. Justo, Z. Wu, C. R. S. da Silva, D. A. Yuen, and D. Kohlstedt, PNAS **106**, 8447 (2009).